JOURNAL OF GUIDANCE, CONTROL, AND DYNAMICS
Vol. 24, No. 4, July–August 2001

Tethered Robot Casting Using a Spacecraft-Mounted Manipulator

Masahiro Nohmi
Kagawa University, Takamatsu, Kagawa 761-0396, Japan
Dragomir N. Nenchev
Hirosaki University, Hirosaki, Aomori 036-8561, Japan
and
Masaru Uchiyama
Tohoku University, Sendai 980-8579, Japan

A space robot attached to the far end of a tether deployed from a spacecraft is considered. Such a robot can be made to translate freely in space without the need of jet thrust, using tether tension. The tethered robot can be applied to perform a variety of tasks such as grappling a remote object, transporting supplies, servicing a satellite, and so on. A casting strategy is described that is accomplished by means of a manipulator mounted on the spacecraft. The tether is attached to the endpoint of this manipulator. The spacecraft-mounted manipulator generates the necessary initial momentum for the tethered robot and adjusts its trajectory by controlling tether tension. The desired final state of the tethered robot includes accurate positioning at the destination point with zero momenta. To achieve such a state, a cooperative control scheme for translation and link motion of the tethered robot is proposed. The effectiveness of the proposed control approach is confirmed by computer simulations.

I. Introduction

TETHERED satellite systems (TSS) offer various attractive potential applications in space, and therefore, they have been an object of study for over two decades.[1–3] In these studies, the tether extension strategy utilizes the gravity force and/or the centrifugal force associated with the orbital motion. Typically, it is assumed that the tether is to be extended for about 20–100 km along the local vertical. Mass, elasticity, and deflection of the tether cannot be neglected in such a case. The TSS is then characterized by various dynamic effects including three-dimensional rigid-body dynamics, swinging and vibrational in-plane and out-of-plane motions of the tether, transverse vibrations of the main satellite, and so on.[2] Because of these diverse dynamic effects, the TSS can become unstable. Therefore, at an early stage, active tether tension control

Masahiro Nohmi received his B.S. in engineering and M.S. in engineering degrees from Keio University, Yokohama, Japan, in 1991 and 1993, and Ph.D. degree from Tohoku University, Sendai, Japan, in 1998, respectively. From 1998 to 2000, he worked on an Engineering Test Satellite VII project as a postdoctoral researcher at the National Aerospace Laboratory. In April 2000 he was appointed as associate professor at the Department of Intelligent Mechanical Systems Engineering, Kagawa University, Kagawa, Japan. His research interests include dynamics and motion control of space robot and tether systems.

Dragomir N. Nenchev received his B.S. in engineering, M.S. in engineering, and Ph.D. degrees from the Technical University of Sofia, Bulgaria in 1979, 1981, and 1985, respectively. He has been with the Robotics Department at the same institution, with the Department of Aeronautics and Space Engineering of Tohoku University and the Department of Mechanical and Production Engineering of Niigata University, Japan. In April 1999 he was appointed professor at the Department of Intelligent Machines and System Engineering, Hirosaki University, Japan. His research interests include kinematics, dynamics, and motion control of underactuated, parallel, and redundant robot systems.

Masaru Uchiyama received his B.S. in engineering, M.S. in engineering, and Ph.D. degrees from the University of Tokyo, Tokyo, Japan, in 1972, 1974, and 1977, respectively, all in mechanical engineering for production. Since 1977, he has been with the School of Engineering, Tohoku University, Sendai, Japan and currently is a Professor of the Space Machines Laboratory, Department of Aeronautics and Space Engineering. He is a recipient of eight paper awards from different academic societies, and since April 1999, is a Visiting Professor at the Institute of Space and Astronautical Science, Japan. His research interests include robotics and its application to aerospace engineering.

Received 12 August 2000; revision received 10 October 2000; accepted for publication 23 November 2000.

has been recognized to be indispensable.[4] Since then, various control approaches have been proposed, including both linear regulators[5] and nonlinear control methods.[6] Also, control strategies employing thrusters, tension in the tether line, or motion of the offset of the tether attachment point have been investigated.[2]

In this paper we propose a new type of TSS. It differs significantly from the TSS studied so far, mainly in three aspects. First, we assume that the tether is to be extended for a relatively short distance, a few hundred meters or so. Second, we do not envision gravity force and/or centrifugal force influencing tether extension. Rather, we will employ a momentum-assisted tether extension strategy. That is, the initial momentum for the tethered subsystem is generated by means of a manipulator arm mounted on the main satellite (spacecraft). The tether itself is attached to the endpoint of this manipulator. In addition, the manipulator arm is also used to control the tension in the tether. Third, we envision the tethered subsatellite to be a multibody system, representing a tethered space robot.

A major consequence of the described momentum-assisted strategy is that the tether can be extended in any direction, not just along the local vertical. We will refer to such a TSS as a tethered space robot, and the momentum-assisted strategy will be referred to as a casting strategy. Expected applications of the tethered space robot include support of space structure construction, servicing a satellite, and others.

Another major consequence of the multibody nature of the subsatellite is that its attitude can be controlled during translation by its own link motion. This can be done by employing methods borrowed from free-flying space robots studies, for example, the virtual manipulator approach[7] or the generalized Jacobian-matrix-based approach.[8,9]

The aim of this paper is to describe a casting strategy for the tethered robot and to propose an appropriate control approach. The following three basic control subtasks are envisioned: 1) trajectory adjustment control subtask via the manipulator arm on the spacecraft (to control the translation to the destination point), 2) tether attachment point control subtask via the tethered robot (subsatellite) link motion (to control the angular momentum), and 3) tethered robot end-effector control subtask (to control the end effector of the tethered robot when performing various activities, such as construction, servicing, etc.).

The paper is organized as follows. Section II introduces the casting strategy and a proper analytical model. Trajectory adjustment control is described in Sec. III. A tether attachment point control formalism is proposed in Sec. IV, which considers the end-effector control. Finally, in Sec. V, we examine the motion of the tethered robot under the proposed control approach via computer simulations.

II. Casting Model

A. Casting Strategy

The casting strategy proposed here comprises three phases (see Fig. 1): In phase I the initial momentum of the tethered robot is generated using the spacecraft-mounted manipulator, in phase II the tethered robot takes off from the spacecraft, and in phase III the tethered robot translates to the destination point.

During casting phases I and II, the tethered robot is rigidly attached to the endpoint of the spacecraft-mounted manipulator. Therefore, the system is controlled according to well-known spacecraft-mounted manipulator control techniques. On the other hand, the control during phase III is quite specific. The tethered robot can be translated to the destination point due to the initial momentum attained in phase I, and it can be stopped at the destination point by tether tension control that is accomplished via endpoint position control of the spacecraft-mounted manipulator.

B. Analytical Model

The main assumptions are as follows.

1) External forces, including the force of gravity, can be neglected.

2) The effect of the orbital motion of the spacecraft is negligible, and the motion of the tethered robot can be described assuming the spacecraft-fixed frame to be inertial.

3) The tether can be modeled as a rigid link.

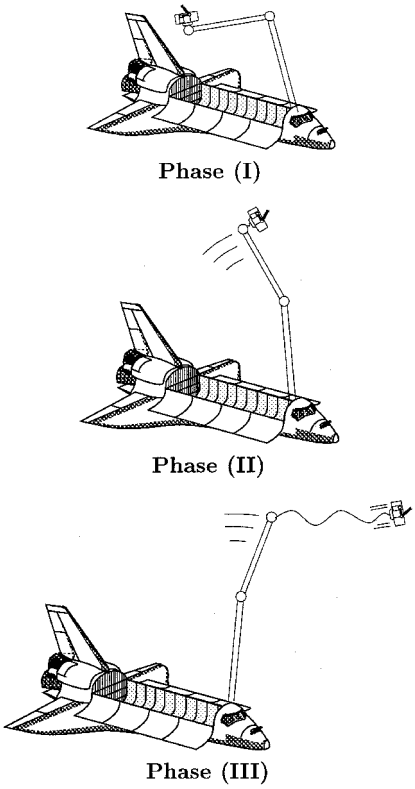

Fig. 1 Casting phases.

4) The tethered robot can be regarded as a system of $n+1$ rigid bodies connected through rotational joints.

The motivation behind the assumptions is as follows. First, we emphasize that the length of the tether is relatively short. Hence, the duration of the casting mission will be small. In other words, the influence of gravity, centrifugal forces due to orbital motion, and other external forces during the relatively short time interval will be small compared to the main forces (tether tension and that due to the tethered robot link motion). For example, let us consider a tethered robot system with an orbital radius of 1×10^4 km, a destination point of 100 m away from the spacecraft (in the tangential direction to the orbit), and a desired mission time for casting of about 100 s. With these data, the positioning error of the tethered robot due to the neglect of gravity gradient, and so on, is estimated to be just about 0.12 m. This error can be easily compensated for.

Second, because the tether is relatively short, and because it is extended due to an initial momentum, the system dynamics are not so complex as in the case of a conventional TSS. The initial momentum ensures that tension is always present during casting, and hence, the tether can be modeled as a rigid link of negligible mass.

The system model is shown in Fig. 2. The inertial frame Σ_I is chosen such that the x axis is parallel to the desired trajectory. The position vectors of the endpoint of the spacecraft-mounted manipulator, of the tether attachment point of the tethered robot, and of the destination point are $\boldsymbol{s}_e$, $\boldsymbol{s}_0$, and $\boldsymbol{d}$, respectively. The tether tension vector is $\boldsymbol{F}$. Body 0 is attached to the tether and will be called the tethered body. Joint i connects body $i-1$ to body i ($i = 1, \ldots, n$). Body n is the end effector. The position vector of the mass center and the angular velocity of body i are $\boldsymbol{s}_i$ and $\boldsymbol{\omega}_i$, respectively and m_i and $\boldsymbol{I}_i$ are the mass and the inertia tensor of body i, respectively. Also, the total mass of the tethered robot and its mass center position vector are, respectively,

$$w = \sum_{i=0}^{n} m_i, \qquad \boldsymbol{s}_g = \sum_{i=0}^{n} \frac{m_i \boldsymbol{s}_i}{w}$$

Here ϕ is the joint variable vector. All 3-vectors are expressed in the Σ_I frame, and their components are denoted by subscripts x, y, and z.

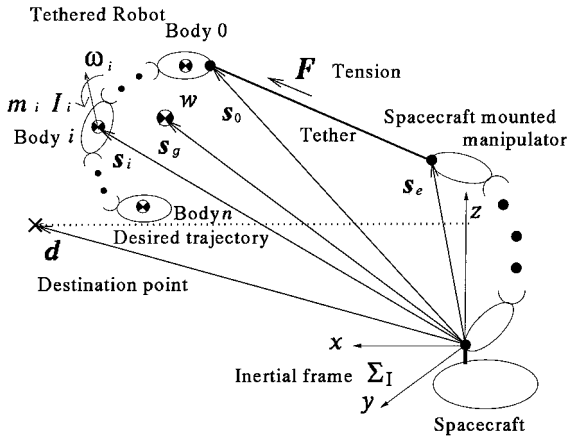

Fig. 2 Casting model of the tethered robot.

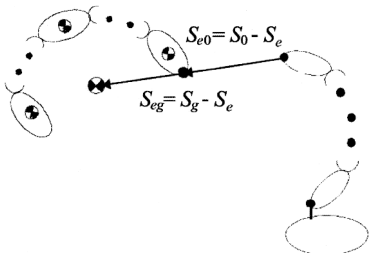

Fig. 3 Condition of the tether attachment point on the connection line.

III. Control for Translation

A. Trajectory Adjustment Control

Trajectory adjustment control has been designed under the assumption that tether tension acts approximately at the mass center of the tethered robot. To satisfy such an assumption, the tether attachment point has to be located on the connection line (Fig. 3), which is along vector $\boldsymbol{s}_{eg}$ ($\equiv \boldsymbol{s}_g - \boldsymbol{s}_e$). Then the motion of the mass center by the tether tension is expressed as

$$w\ddot{\boldsymbol{s}}_g = \boldsymbol{F} \tag{1}$$

Deviation of the tether attachment point from the connection line is discussed in Sec. IV.C. Because the x axis of the Σ_I frame is parallel to the desired trajectory, the tethered robot can be stopped at the destination point only with proper control of F_x when the mass center translates along the desired path. On the other hand, F_y and F_z are needed for path adjustment, when the mass center of the tethered robot deviates from the desired path due to disturbances. Because of this choice of the Σ_I frame orientation, a decoupled control law can be designed: F_x is used to control the rate of approach to the destination point; F_y and F_z are used to adjust the deviation from the desired path.

The governing geometrical relation

$$\boldsymbol{F}/\|\boldsymbol{F}\| = \boldsymbol{s}_{e0}/\|\boldsymbol{s}_{e0}\| \tag{2}$$

can be written as

$$\frac{1}{s_{e0x}}\begin{bmatrix} s_{e0y} \\ s_{e0z} \end{bmatrix} = \frac{1}{F_x}\begin{bmatrix} F_y \\ F_z \end{bmatrix} \tag{3}$$

where $\boldsymbol{s}_{e0} \equiv \boldsymbol{s}_0 - \boldsymbol{s}_e$. To compensate a deviation of the tethered robot from the desired path, we introduce the following proportional and derivative control:

$$w\begin{bmatrix} \ddot{s}_{gy} \\ \ddot{s}_{gz} \end{bmatrix} = -\boldsymbol{K}_v\begin{bmatrix} \dot{s}_{gy} \\ \dot{s}_{gz} \end{bmatrix} - \boldsymbol{K}_p\begin{bmatrix} s_{gy} - d_y \\ s_{gz} - d_z \end{bmatrix} \tag{4}$$

where $\boldsymbol{K}_v$ and $\boldsymbol{K}_p$ are control gains.

Note that F_y and F_z depend mainly on s_{ey} and s_{ez} and that s_{ex} does not influence the direction of tether extension significantly. Then, from Eqs. (1–4), the endpoint of the spacecraft mounted manipulator should be located at

$$\begin{bmatrix} s^c_{ey} \\ s^c_{ez} \end{bmatrix} = \begin{bmatrix} s_{0y} \\ s_{0z} \end{bmatrix} - \frac{s_{0x} - s^c_{ex}}{F^d_x}\left\{\boldsymbol{K}_v\begin{bmatrix} \dot{s}_{gy} \\ \dot{s}_{gz} \end{bmatrix} + \boldsymbol{K}_p\begin{bmatrix} s_{gy} - d_y \\ s_{gz} - d_z \end{bmatrix}\right\} \tag{5}$$

under the condition that F^d_x and s^c_{ex} are known, where $(\,)^d$ and $(\,)^c$ are the desired and a commanded value of $(\,)$, respectively. Note that the tether tension vector cannot be commanded because $\boldsymbol{F}$ will be determined by $\|\boldsymbol{F}\|$ and $\boldsymbol{s}_e$.

B. Translation Control Efficiency

Because the trajectory adjustment control can be decoupled in the y and z directions, we select the control gains in Eq. (4) as

$$\boldsymbol{K}_v = \mathrm{diag}[k_v, k_v], \qquad \boldsymbol{K}_p = \mathrm{diag}[k_p, k_p]$$

In the presence of disturbances along the y and z axes, Eq. (4) is rewritten as

$$w\begin{bmatrix} \ddot{s}_{gy} \\ \ddot{s}_{ez} \end{bmatrix} + k_v\begin{bmatrix} \dot{s}_{gy} \\ \dot{s}_{gz} \end{bmatrix} + k_p\begin{bmatrix} s_{gy} - d_y \\ s_{gz} - d_z \end{bmatrix} = \begin{bmatrix} \delta_y \\ \delta_z \end{bmatrix} \tag{6}$$

where δ_y and δ_z are the disturbances. For the purpose of examining the characteristics of Eq. (6), it is assumed that δ_y and δ_z are impulsive disturbances occurring at time $t_\delta = 0$. To satisfy Eq. (6), tether tension must be

$$\begin{bmatrix} F^d_y \\ F^d_z \end{bmatrix} = -\frac{2}{\tau}\left(1 - \frac{t_\delta}{2\tau}\right)e^{-t_\delta/\tau}\begin{bmatrix} \delta_y \\ \delta_z \end{bmatrix} \tag{7}$$

where $\tau = k_v/2k_p$.

On the other hand, any F_x for trajectory control is admissible because the direction of the tether extension is almost along the x axis. However, F_y and F_z are limited geometrically by the workspace of the spacecraft-mounted manipulator. From Eq. (3), it becomes apparent that the admissible tether tension decreases with a growing distance from the spacecraft to the tethered robot. Also, s_{ex} should be selected such that $s^{\max}_{ey}$ and $s^{\max}_{ez}$ become large because those values determine the geometrical limitations on F_y and F_z. Note, $(\,)^{\max}$ is the admissible maximum value of $(\,)$.

Sample numerical results for the y direction, the maximum tension $F^{\max}_y$ determined from Eq. (3), and the required tension F^d_y obtained from Eq. (7) are shown in Fig. 4. For Eq. (3), the parameters are set as $F_x = 2$ N, $w = 100$ kg, $s_{ex} = 0$ m, and $s^{\max}_{ey} = 2$ m, and $\ddot{s}_{gx} = F_x/w$, $s_{gy} = 0$, $\boldsymbol{s}_g = \boldsymbol{s}_0$ are assumed. To solve Eq. (7), $k_v = 2\omega$, $k_p = \omega^2$, and $\delta_y = 1/\omega$ Ns (at $t_\delta = 0$).

The solid line stands for $|F^{\max}_y|$. $|F^d_y|$ is displayed by a dotted line when $\omega = 0.2$ 1/s, by a dashed line when $\omega = 0.3$ 1/s, and by a chained line when $\omega = 0.4$ 1/s. From these results it is clear that trajectory adjustment is possible when $\omega = 0.3, 0.4$ 1/s. On the contrary, it will be impossible when $\omega = 0.2$ 1/s for a certain interval of time Δt, as indicated in Fig. 4. As a consequence, we can conclude that small control gains can compensate for large disturbances ($\delta_y = 1/\omega$); however, when the gains become too small, trajectory adjustment control becomes inefficient.

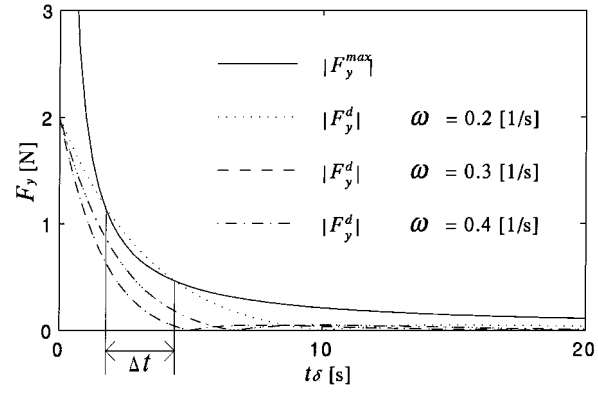

Fig. 4 Required and maximum tether tension.

IV. Control of Angular Momentum

A. Rotation of the Tethered Robot

It should be apparent that a rotational motion of the tethered robot with respect to its mass center will be inevitable. This is because tether tension does not act exactly at the mass center of the tethered robot. Then, we can expect that the angular momentum of the tethered robot with respect to its mass center will change due to the torque generated by the tether tension. Therefore, in addition to trajectory adjustment control, angular momentum control is also required.

The torque $\boldsymbol{N}$ caused by tether tension can be written as

$$\boldsymbol{N} = \tilde{\boldsymbol{s}}_{0g}\boldsymbol{F} = (\|\boldsymbol{F}\|/\|\boldsymbol{s}_{e0}\|)\tilde{\boldsymbol{s}}_{0g}\boldsymbol{s}_{e0} = (\|\boldsymbol{F}\|/\|\boldsymbol{s}_{e0}\|)\tilde{\boldsymbol{s}}_{0g}\boldsymbol{s}_{eg} \tag{8}$$

where $\boldsymbol{s}_{0g} \equiv \boldsymbol{s}_g - \boldsymbol{s}_0$, $\boldsymbol{s}_{eg} \equiv \boldsymbol{s}_g - \boldsymbol{s}_e$, and $\tilde{\ }$ denotes the skew-symmetric cross-product matrix of ( ). Equation (8) shows that the torque caused by tether tension depends on the position of the tether attachment point. Therefore, the angular momentum of the tethered robot can be controlled via position control of the tether attachment point, which, in turn, is done via link motion control of the tethered robot. Also note from Eq. (8) that $\boldsymbol{N}$ is located in the plane normal to the connection line. This means that in the direction of the connection line no torque will be generated by tether tension; to control angular momentum in this direction, a reaction wheel or a jet thruster has to be employed. Then, under the desired condition that $\boldsymbol{s}_{e0}$ is parallel to the x axis, the respective angular momentum components in the y and z axes will be controllable, by applying torque components N_y and N_z.

B. Momenta of the Tethered Robot

In contrast to fixed-base robots, the linear and angular momenta of a robot with a floating base, such as a tethered robot, play an important role. Total momenta, denoted by the summation of each body momenta of the tethered robot with respect to the Σ_I frame, are

$$\begin{bmatrix}\boldsymbol{P}_s\\ \boldsymbol{L}_s\end{bmatrix} = \boldsymbol{H}_0\begin{bmatrix}\dot{\boldsymbol{s}}_0\\ \boldsymbol{\omega}_0\end{bmatrix} + \boldsymbol{H}_\phi\dot{\boldsymbol{\phi}} + \begin{bmatrix}\boldsymbol{0}\\ \tilde{\boldsymbol{s}}_0\boldsymbol{P}_s\end{bmatrix} \tag{9}$$

where

$$\boldsymbol{H}_0 = \begin{bmatrix} w\boldsymbol{E} & w\tilde{\boldsymbol{s}}_{0g}^T \\ w\tilde{\boldsymbol{s}}_{0g} & \sum_{i=0}^{n}\{\boldsymbol{I}_i + m_i\tilde{\boldsymbol{s}}_{0i}^T\tilde{\boldsymbol{s}}_{0i}\} \end{bmatrix}$$

$$\boldsymbol{H}_\phi = \begin{bmatrix} \sum_{i=1}^{n} m_i\boldsymbol{J}_{Li} \\ \sum_{i=1}^{n}\{\boldsymbol{I}_i\boldsymbol{J}_{Ai} + m_i\tilde{\boldsymbol{s}}_{0i}\boldsymbol{J}_{Li}\} \end{bmatrix}$$

$i = 0, 1, \ldots, n$, $\boldsymbol{E}$ is the unit matrix of respective dimension, and $\boldsymbol{s}_{0i} \equiv \boldsymbol{s}_i - \boldsymbol{s}_0$,

$$\boldsymbol{J}_{Li} = \begin{bmatrix}\tilde{\boldsymbol{k}}_1(\boldsymbol{r}_i - \boldsymbol{p}_1) & \cdots & \cdots & \tilde{\boldsymbol{k}}_i(\boldsymbol{r}_i - \boldsymbol{p}_i) & \boldsymbol{0}_{3\times(n-i)}\end{bmatrix} \in \Re^{3\times n}$$

$$\boldsymbol{J}_{Ai} = \begin{bmatrix}\boldsymbol{k}_1 & \cdots & \boldsymbol{k}_i & \boldsymbol{0}_{3\times(n-i)}\end{bmatrix} \in \Re^{3\times n}$$

where $\boldsymbol{0}_{j\times k} \in \Re^{j\times k}$, $\boldsymbol{p}_j$ is the position vector from the tether attachment point to joint j ($j, k = 1, 2, \ldots$), and $\boldsymbol{k}_i$ is the unit vector along the rotational axis of joint i. The mass center momenta of the tethered robot with respect to the Σ_I frame can be written as

$$\begin{bmatrix}\boldsymbol{P}_m\\ \boldsymbol{L}_m\end{bmatrix} = w\begin{bmatrix}\boldsymbol{E}\\ \tilde{\boldsymbol{s}}_g\end{bmatrix}\dot{\boldsymbol{s}}_g \tag{10}$$

The difference between the momenta in Eqs. (9) and (10) is

$$\mathcal{L}_r \equiv \begin{bmatrix}\boldsymbol{0}\\ \boldsymbol{L}_r\end{bmatrix} = \boldsymbol{H}_0\begin{bmatrix}-\dot{\boldsymbol{s}}_{0g}\\ \boldsymbol{\omega}_0\end{bmatrix} + \boldsymbol{H}_\phi\dot{\boldsymbol{\phi}} \tag{11}$$

where $\boldsymbol{L}_r$ is angular momentum of the tethered robot, which is a sum of each body's angular momentum with respect to the tethered robot mass center. From the last Eq. (11) we have

$$\boldsymbol{P}_r \equiv \boldsymbol{P}_s = \boldsymbol{P}_m \tag{12}$$

where $\boldsymbol{P}_r$ is translational momentum of the tethered robot.

C. Tether Attachment Point Control

Denote the y and z components of the vector cross product in the right-hand side of Eq. (8) as

$$\begin{bmatrix}\lambda_y\\ \lambda_z\end{bmatrix} \equiv \frac{1}{\|\boldsymbol{s}_{e0}\|}\begin{bmatrix}s_{0gz}s_{egx} - s_{0gx}s_{egz}\\ s_{0gx}s_{egy} - s_{0gy}s_{egx}\end{bmatrix} \tag{13}$$

Note that the limit values for the generated torque depend on both tether tension and the workspace of the tether attachment point. Tether tension is determined from the trajectory adjustment control (see Sec. III.A). Therefore, we consider the desired value of λ_y and λ_z as

$$\begin{bmatrix}\lambda_y^d\\ \lambda_z^d\end{bmatrix} = \zeta_\lambda\begin{bmatrix}L_{ry}\\ L_{rz}\end{bmatrix} \tag{14}$$

where ζ_λ is a control gain.

We consider a velocity command generator-type controller for the link motion. First, define the following extended task-space vector

$$\boldsymbol{\nu} \equiv \begin{bmatrix}\boldsymbol{\nu}_e\\ \dot{\lambda}_x\\ \dot{\lambda}_y\end{bmatrix} = \boldsymbol{J}_{st}\begin{bmatrix}-\dot{\boldsymbol{s}}_{0g}\\ \boldsymbol{\omega}_0\end{bmatrix} + \boldsymbol{J}_{mt}\dot{\boldsymbol{\phi}} \tag{15}$$

where $\boldsymbol{\nu}_e$ is the end-effector motion velocity and

$$\boldsymbol{J}_{st} \equiv \begin{bmatrix}\boldsymbol{J}_s\\ \boldsymbol{J}_\lambda\end{bmatrix}, \qquad \boldsymbol{J}_{mt} \equiv \begin{bmatrix}\boldsymbol{J}_m\\ \boldsymbol{0}_{2\times n}\end{bmatrix}$$

$\boldsymbol{J}_s$ and $\boldsymbol{J}_m$ are the tethered body motion and the fixed-base manipulator Jacobian matrices for $\boldsymbol{\nu}_e$, respectively, and

$$\boldsymbol{J}_\lambda \equiv \frac{1}{\|\boldsymbol{s}_0\|}\begin{bmatrix}s_{egz} & 0 & -s_{egx} & \boldsymbol{0}_{2\times 3}\\ -s_{egy} & s_{egz} & 0\end{bmatrix}$$

Because the endpoint of the spacecraft-mounted manipulator and the mass center position of the tethered robot cannot be controlled by the link motion, in deriving Eq. (15) we assume that

$$\boldsymbol{s}_{eg}/\|\boldsymbol{s}_{e0}\| = \text{const} \tag{16}$$

Substituting Eq. (11) into Eq. (15), we obtain

$$\boldsymbol{\nu} = \boldsymbol{J}_g\dot{\boldsymbol{\phi}} + \boldsymbol{J}_{st}\boldsymbol{H}_s^{-1}\mathcal{L}_r \tag{17}$$

where

$$\boldsymbol{J}_g \equiv \boldsymbol{J}_{mt} - \boldsymbol{J}_{st}\boldsymbol{H}_s^{-1}\boldsymbol{H}_m$$

is the generalized Jacobian matrix (see Ref. 8). To this end, we can briefly summarize that the control objective is to obtain proper link motion to ensure simultaneous accomplishment of two tasks: a main task for the end-effector motion control and an auxiliary task, which we identified as a tether attachment point control task.

D. Cooperative Control

Note that there is a coupling between the trajectory adjustment control subtask and the tether attachment point control subtask. Indeed, Eq. (2) clearly shows that tether tension is related to the position of the tether attachment point. Also note that tether attachment point control implies that the tether attachment point will necessarily deviate from the connection line, and hence, tether tension will not act exactly at the mass center of the tethered robot. As a consequence, trajectory adjustment control cannot be

performed accurately. For the tether attachment point control, the tether attachment point should be operated in the plane normal to the angular momentum vector (Fig. 5). Then, the error of trajectory adjustment control due to rotational motion of the tethered robot is also in that plane. Therefore, it can be said that the trajectory adjustment control and the tether attachment point control involve planar coupling. In other words, three-dimensional momentum control is required for casting; however, translational and angular momentum are coupled in two-dimensional space.

The control block diagram for the cooperative control is shown in Fig. 6. For the trajectory adjustment control, position and velocity of the tethered robot mass center $\boldsymbol{s}_g$ and $\dot{\boldsymbol{s}}_g$ and the endpoint position for the spacecraft-mounted manipulator $\boldsymbol{s}_e$ are assumed to be measured. Then, tether tension input $\|\boldsymbol{F}^d\|$ and the endpoint position input $\boldsymbol{s}_e^c$ can be calculated, referring to the command s_{ex}^c. On the other hand, joint angles $\boldsymbol{\phi}$, position of the mass center $\boldsymbol{s}_g$, and angular momentum $\boldsymbol{L}_r$ are assumed to be measured, for the purpose of the tether attachment point control. Then, referring to the end-effector motion velocity command $\boldsymbol{\nu}_e$, joint angle velocities $\dot{\boldsymbol{\phi}}$ can be calculated.

V. Simulation

A. Simulation Parameters

As described in Sec. I, tethered robot casting is feasible when the distance of translation is short enough, so that gravity gradient and orbital centrifugal effect can be neglected. In the simulation, the purpose of the proposed control is that the tethered robot translates to the destination point with the allowable margin of the mentioned error; hence, gravity and orbital centrifugal force can be neglected.

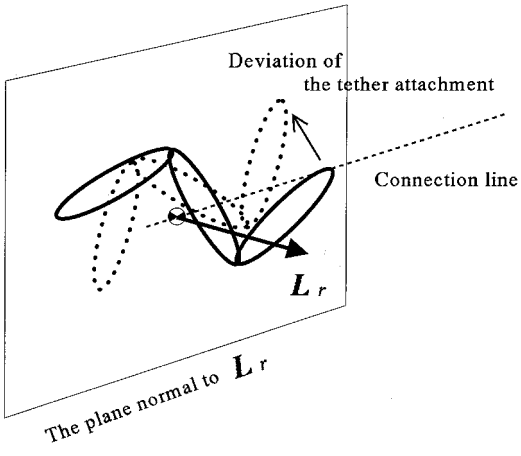

Fig. 5 Controls coupling in plane.

In the simulation, we will employ the following computed torque method for the endpoint control of the large spacecraft mounted manipulator:

$$\boldsymbol{\tau} = \boldsymbol{h} + \boldsymbol{M}\boldsymbol{J}_c^{-1}[-\dot{\boldsymbol{J}}_c\,\dot{\boldsymbol{q}} + \boldsymbol{u}] \tag{18}$$

$$\boldsymbol{u} = \boldsymbol{C}_v\left(\dot{\boldsymbol{s}}_e^c - \dot{\boldsymbol{s}}_e\right) + \boldsymbol{C}_p\left(\boldsymbol{s}_e^c - \boldsymbol{s}_e\right) \tag{19}$$

where $\boldsymbol{h}$, $\boldsymbol{M}$, $\boldsymbol{J}_c$, and $\boldsymbol{q}$ are the Coriolis and centrifugal forces of the manipulator motion, matrix of inertia, the Jacobian, and the joint variable vector, respectively, and $\boldsymbol{\tau}$ is a joint torque vector. The control error due to the preceding control law is regarded as a disturbance during casting. The control gains are set as

$$\boldsymbol{C}_v = 2\boldsymbol{E}\ \text{1/s}, \qquad \boldsymbol{C}_p = \boldsymbol{E}\ \text{1/s}^2$$

then any deviation can be damped out by setting $\dot{\boldsymbol{s}}_e^c = \boldsymbol{0}$ in Eq. (19). Here, $\boldsymbol{s}_e$ deviates from $\boldsymbol{s}_e^c$, especially when a force is applied at the endpoint by inertia due to the mass of the tethered robot and tether tension. Such a force is larger in phase I than that in phase III, because the time for accelerating the tethered robot is shorter than that for stopping it. Therefore, the endpoint error in phase I will be an initial disturbance for casting of the tethered robot.

Because of the cooperative control planar coupling, as described in Sec. IV.C, the simulation model becomes a two-dimensional one (in the xz plane on the Σ_I frame). Given values are commanded position of the endpoint of the spacecraft-mounted manipulator and the commanded velocity of the tethered robot. The commanded velocity $\dot{\phi}^c$ is derived from Eq. (17), using the following task vector:

$$\boldsymbol{\nu}^c = \begin{bmatrix} \boldsymbol{\nu}_e \\ \dot{\lambda}_y \end{bmatrix} = \begin{bmatrix} \Phi_n^c - \Phi_n \\ \lambda_y^d - \lambda_y \end{bmatrix} \tag{20}$$

where $\Phi_n\ (\equiv \Phi_0 + \phi_1 + \cdots + \phi_n)$ denotes the attitude of the end-effector, which is a scalar in the xz plane. Φ_0 is the tethered body attitude, which is also a scalar, and ϕ_i, $i = 1, 2, \ldots, n$, is the ith joint angle, respectively. The control gain for the angular momentum control is set as $\zeta_\lambda = 0.2$; then, the tether attachment point motion is always located in the tethered robot workspace of the simulation model. When the numerical results in Sec. III.B are referred to, control gains in Eq. (4) are $k_v = 0.6$ 1/s and $k_p = 0.9$ 1/s^2. To control the approach of the tethered robot to the destination point, F_x^d is given as

$$F_x^d = w\frac{\dot{s}_{gx}^2}{2(s_{gx} - d_x)} \tag{21}$$

F_z^d is obtained from the right hand of Eq. (4) for path adjustment. Then, tether tension is applied as

$$\|\boldsymbol{F}^d\| = \sqrt{\left(F_x^d\right)^2 + \left(F_z^d\right)^2} \tag{22}$$

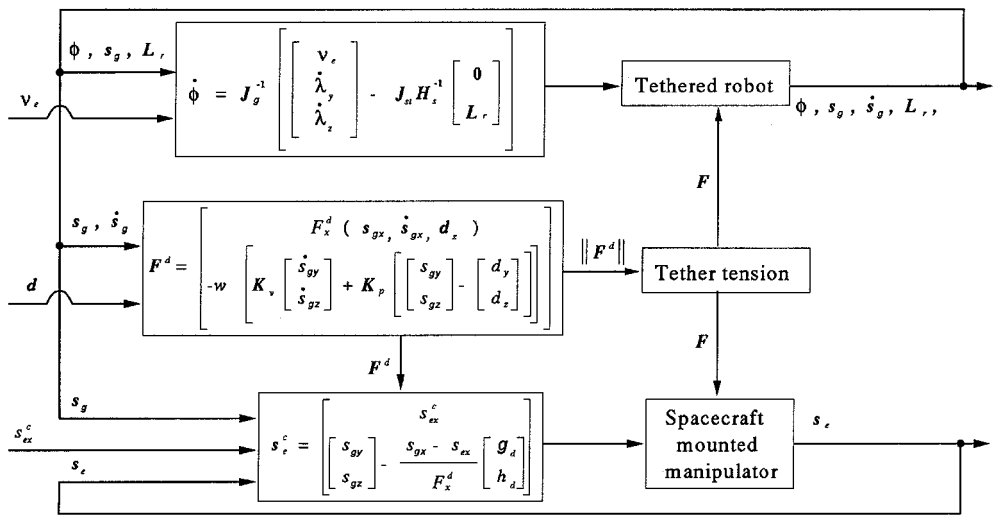

Fig. 6 Control block diagram.

Each body of the spacecraft-mounted manipulator and the tethered robot is assumed to be a thin rod with uniform inertia. The spacecraft-mounted manipulator system consists of two manipulator links. The length, mass, and moment of inertia of the ith link are l_{ci}, m_{ci}, and I_{ci}, respectively, $i = 1, 2$. The tethered robot consists of three links connected with two rotational joints ($n = 2$). Therefore, the arm of the tethered robot has two degrees of freedom (DOF). The number of DOF has been selected to guarantee the end-link attitude control task and the tether attachment point control task. The spacecraft-mounted manipulator and the tethered robot parameters are $l_{ci} = 2$ m, $m_{ci} = 10$ kg, $I_{ci} = 20$ kgm^2, $l_0 = l_1 = l_2 = 1$ m, $m_0 = m_1 = 30$ kg, $m_2 = 40$ kg, $I_0 = I_1 = 30$ kgm^2, and $I_2 = 40$ kgm^2, respectively.

B. Initial Conditions for Casting

The destination point is set as $(d_x, d_z) = (100, 2)$ m. A set of initial conditions for phase I is given as $(s_{ex}, s_{ez}) = (-1, 2)$ m, $\Phi_0 = 0$ rad, $\dot{\Phi}_0 = 0$ rad/s, $\phi_i = 0$ rad, and $\dot{\phi}_i = 0$ rad/s, where $i = 1, 2$. The initial conditions of the tethered robot Φ_0, $\dot{\Phi}_0$ and ϕ_i, $\dot{\phi}_i$ are maintained by phase II. The desired condition for the spacecraft-mounted manipulator at phase II is set as $(s_{ex}, s_{ez}) = (0, 2)$ m, and $(\dot{s}_{ex}, \dot{s}_{ez}) = (2, 0)$ m/s, and the endpoint is controlled as constant acceleration during phase I. A set of results in phase II is shown on Table 1, where $s_{ex} = s_{0x}$ and $s_{ez} = s_{0z}$. Under this condition in phase II, the tethered robot will deviate from the desired trajectory in phase III. On the other hand, the endpoint of the spacecraft-mounted manipulator will deviate from the desired position as soon as the tethered robot takes off, which is also the main error of the desired mission.

C. Simulation Results

The following two cases during phase III have been simulated: case 1, $\boldsymbol{\nu}^c = \mathbf{0}$, and case 2, $\boldsymbol{\nu}^c = [\boldsymbol{\nu}_e^T \;\; \dot{\lambda}_y]^T$, with $s_{ex}^c = 0$ m in both cases. The time at phase II is set at $t = 0$ s. Figures 7 and 8 show the time history of $\boldsymbol{s}_e$ (the endpoint of the spacecraft-mounted manipulator) and $\boldsymbol{s}_g$ (the mass center of the tethered robot), respectively. Figure 9 shows time histories of the translational momentum P_r ($=\|\boldsymbol{P}_r\|$), the angular momentum L_r ($=\|\boldsymbol{L}_r\|$), and the end-effector attitude Φ_2, respectively.

In Fig. 7, it is seen that, initially, after the tethered robot has taken off, the endpoint motion of the spacecraft-mounted manipulator is relatively large. The reason is that large disturbances have occurred during the takeoff phase II. On the other hand, note that after a while the endpoint motion is stabilized. This is in spite of an existing disturbance due to tether tension (tether tension is never zero during the translational motion in phase III, as already explained). However,

Table 1 Condition in phase II

Value	s_{ex}, m	s_{ez}, m	$\dot{s}_{ex}$, m/s	$\dot{s}_{ez}$, m/s
Desired	0.00	2.00	2.00	−0.00
Calculated	0.054	2.00	2.02	−0.0057

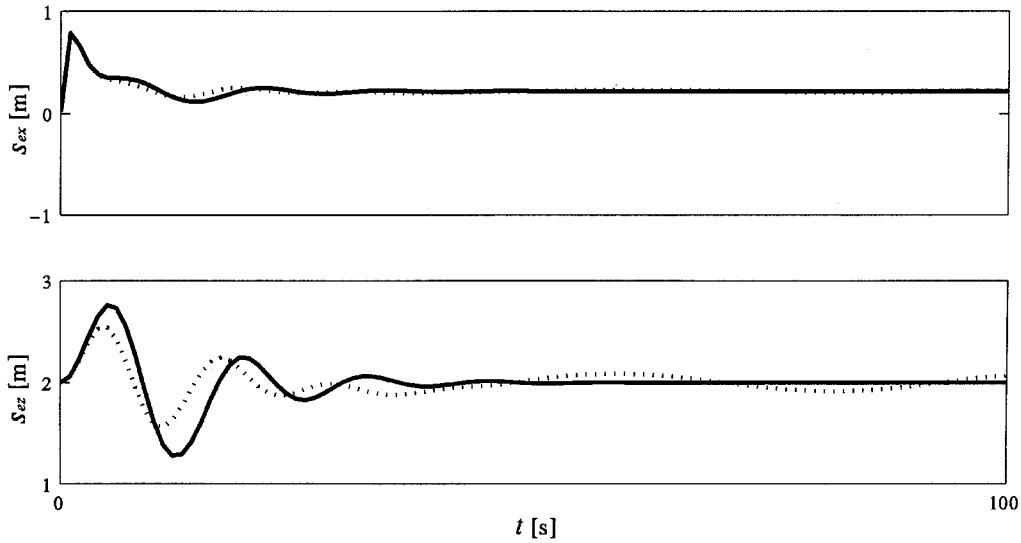

Fig. 7 Endpoint state time history of the spacecraft mounted manipulator: - - - - for case 1, and —— for case 2.

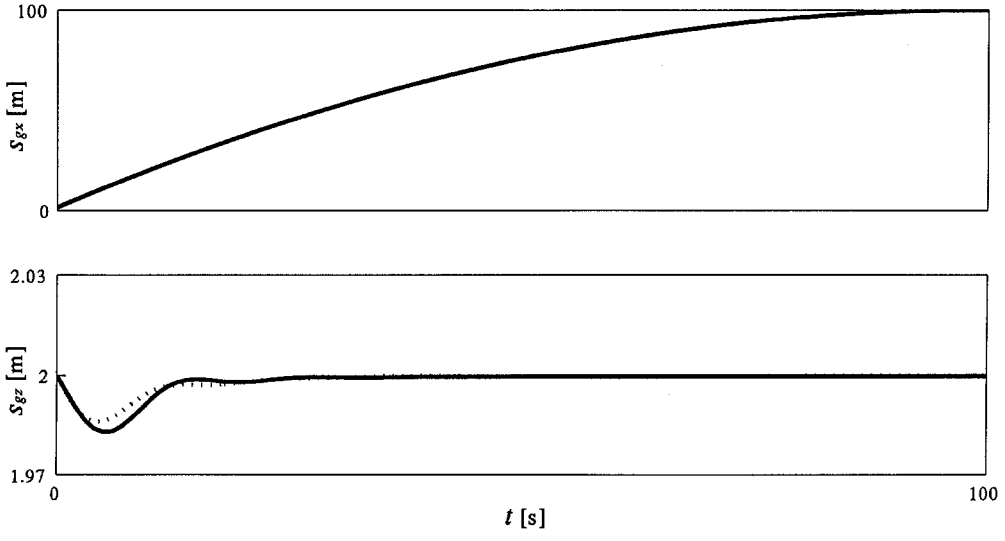

Fig. 8 Mass center state time history of the tethered robot: - - - - for case 1, and —— for case 2.

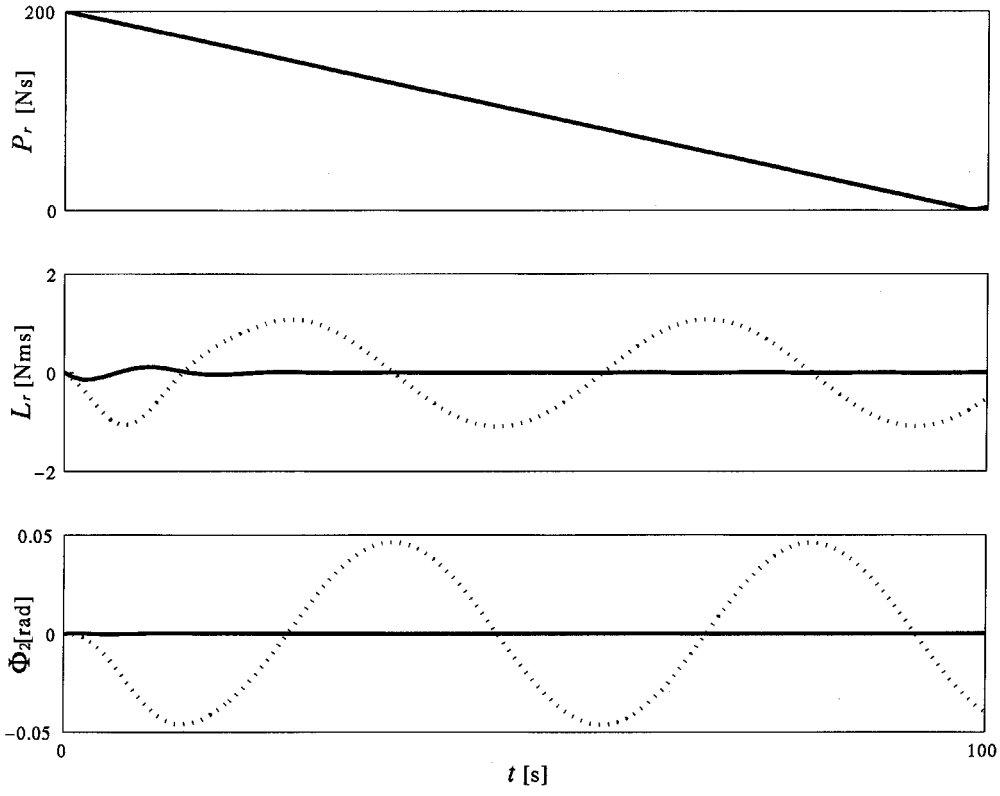

Fig. 9 Momentum and end-effector attitude state time history during tethered robot casting: - - - - for case 1, and —— for case 2.

this disturbance is relatively small and can be easily compensated via the computed torque control law with the small gain $\boldsymbol{C}_v$ and $\boldsymbol{C}_p$ in the simulation.

From Fig. 9, note that the change of the angular momentum in case 2 is smaller than that in case 1, although the changes of translational momentum are same. Also note that the angular momentum of the tethered robot is not zero in case 1, when arriving at the destination point. Therefore, in case 1, the tethered robot performs rotational motion with respect to its mass center at the destination point and cannot stop its motion.

On the other hand, trajectories of the mass center of the tethered robot are slightly different in cases 1 and 2 (Fig. 8). Also, the endpoint motion of the spacecraft-mounted manipulator is different (Fig. 7). The reason is that the tether tension vector deviates from the command for trajectory adjustment due to the tether attachment point control, although the endpoint of the spacecraft-mounted manipulator is located at the commanded position. Such a deviation of the tether attachment point from the connection line is necessary for compensation control of the angular momentum.

VI. Conclusions

We discussed a casting strategy for a tethered space robot using a spacecraft-mounted manipulator. We proposed a cooperative control scheme with regard to the momenta of the tethered robot. Casting strategy is that the spacecraft-mounted manipulator generates initial momentum for the tethered robot and adjusts its trajectory by controlling the tether tension. To achieve the proposed strategy, the trajectory adjustment control was described, and its efficiency was examined. On the other hand, the tether attachment point control of a tethered robot subsystem was proposed, to control the angular momentum, which changes with tether tension variation. Proper control of the tether attachment point enables keeping zero angular momentum with respect to the mass center of the tethered robot. Link motion control of the tethered robot is composed of two subtasks: the tether attachment point motion subtask and the end-effector motion subtask. Computer simulations show the effectiveness of the proposed control approach. Therefore, we can conclude that the tether attachment point control of a tethered robot is effective, despite its influence on trajectory adjustment control.

References

[1] Rupp, C. C., and Laue, J. H., "Shuttle/Tethered Satellite System," *Journal of Astronautical Sciences*, Vol. 26, No. 1, 1978, pp. 1–17.

[2] Modi, V. J., Lakshmanan, P. K., and Misra, A. K., "On the Control of Tethered Satellite Systems," *Acta Astronautica,* Vol. 26, No. 6, 1992, pp. 411–423.

[3] Fujii, H., and Ishijima, S., "Mission-Function Control for Deployment and Retrieval of a Subsatellite," *Journal of Guidance, Control, and Dynamics,* Vol. 12, No. 2, 1989, pp. 243–247.

[4] Rupp, C. C., "A Tether Tension Control Law for Tethered Subsatellite Deployed along Local Vertical," NASA TM X-64963, 1975.

[5] Bainum, P. M., and Kumar, V. K., "Optimal Control of the Shuttle-Tethered-Subsatellite System," *Acta Astronautica,* Vol. 7, No. 6, 1980, pp. 1333–1348.

[6] Pines, D. J., Flotow, A. H., and Redding, D. C., "Tow Nonlinear Control Approaches for Retrieval of a Thrusting Tethered Subsatellite," *Journal of Guidance, Control, and Dynamics,* Vol. 13, No. 4, 1990, pp. 651–658.

[7] Vafa, Z., and Dubowsky, S., "On the Dynamics of Space Manipulators Using the Virtual Manipulator, with Applications to Path Planning," *Journal of Astronautical Sciences,* Vol. 38, No. 4, 1990, pp. 441–472.

[8] Umetani, Y., and Yoshida, K., "Resolved Motion Rate Control of Space Manipulators with Generalized Jacobian Matrix," *IEEE Transactions on Robotics and Automation,* Vol. 5, No. 3, 1989, pp. 303–314.

[9] Masutani, Y., Miyazaki, F., and Arimoto, S., "Sensory Feedback for Space Manipulators," *Proceedings of the 1989 IEEE International Conference on Robotics and Automation,* Vol. 3, IEEE Computer Society Press, Washington, DC, 1989, pp. 1346–1351.